Calculation of $M1$ transition rates at high spin in axial nuclei

Y. S. Chen* and P. B. Semmes
Joint Institute for Heavy Ion Research, Oak Ridge, Tennessee 37831

G. A. Leander
UNISOR, Oak Ridge Associated Universities, Oak Ridge, Tennessee 37831

(Received 30 June 1986)

A method is proposed for applying the cranking model to the calculation of $M1$ transition rates between high spin states. The accuracy is checked by comparing numerical results with recent high-spin data for ^{165}Lu, which provides a critical test, and with a physically equivalent three-quasiparticle plus rotor calculation. The nucleus ^{81}Kr is also considered. The behavior of the $M1$ rates at high spin is qualitatively and semiquantitatively reproduced.

I. INTRODUCTION

The nucleonic spins, and consequently also the nucleonic magnetic dipoles, cancel pairwise in the superfluid ground states of nuclei. Nuclear rotation breaks this pairwise cancellation, and the resulting $M1$ properties provide insight into the microscopic structure of the rotational states. A theory of the microscopic structure at high spin is provided by the cranking model,[1] but its applicability to $M1$ properties has not been established. In recent years a variety of alternative models were proposed to describe $M1$ transition rates between three-quasiparticle states of high spin,[2–4] and results based on cranking were more or less directly implied to be unsatisfactory. However, all the alternative models share a major disadvantage in that they assume a clear separation between a core and a few unpaired quasiparticles. Therefore, unlike the cranking model, they cannot be generalized to very high spin or finite temperature.

In this paper we pave the way for the application of the cranking model to the latter cases by showing that the strong $M1$ transitions observed in some "$\Delta I=1$ bands" at high spins can be fairly well reproduced by the cranking model. This is the kind of strong $M1$ transition that is least accurately described by cranking, and the accuracy is expected to increase in going to higher spins than those considered here.[5]

The essential new feature of the present cranking calculations is that both the rotating quasiparticle $M1$ transition matrix elements and the g factor for the remainder of the nucleus are obtained from the microscopic cranking wave functions. In the previous high-spin calculations of Ref. 6 the g factor was chosen approximately equal to Z/A. This precludes good results for three-quasiparticle yrast states, because the g factor is changed considerably by the rotational alignment of two "spectator quasiparticles" in the S band. The change is taken into account by using the cranking wave functions to calculate g.

The present study deals with the axially symmetric case. The triaxial case will be considered in a forthcoming paper.

II. MODELS

A. The cranking model

The cranking Hamiltonian for nucleonic motion in a rotating mean field with a residual monopole pairing interaction is

$$h^{\omega}=\sum_{\nu}(\epsilon_{\nu}-\lambda)a_{\nu}^{\dagger}a_{\nu}+\tfrac{1}{2}\Delta\sum_{\nu\mu}\delta(\bar{\nu},\mu)(a_{\nu}^{\dagger}a_{\mu}^{\dagger}+a_{\mu}a_{\nu}) -\omega\sum_{\nu\mu}\langle\nu|\hat{j}_x|\mu\rangle a_{\nu}^{\dagger}a_{\mu}\ . \quad (1)$$

Here the $a_{\nu}^{\dagger}$ are creation operators for single-particle states $|\nu\rangle$ in the nonrotating mean field, ϵ_{ν} are the corresponding single-particle energies, $\bar{\nu}$ is the time-reversed orbit, $\hat{j}_x$ is the x component of the single-particle angular momentum operator, and ω is the externally imposed frequency for semiclassical rotation of the mean field about the x axis. The Hamiltonian h^{ω} is diagonalized by a Bogoliubov transition,

$$a_{\nu}=\sum_{i}(A_{\nu}^{i}b_i+B_{\nu}^{i}b_i^{\dagger})\ . \quad (2)$$

The rotating quasiparticle states created by the $b_i^{\dagger}$ operators are $|\alpha\rangle_i$, where the signature quantum number α is $+\frac{1}{2}$ or $-\frac{1}{2}$. The vacuum plus a single rotating quasiparticle in the state $|\alpha\rangle_i$ for a sequence of ω values corresponds to an odd-A rotational band with the spin states $I=2n+\alpha$ (n an integer). For each ω, the shape of the mean field and the gap parameter Δ of the pair field should, in principle, be determined self-consistently, and the Fermi level λ should be adjusted to give the correct average particle number. In the calculations presented below, however, we hold these quantities fixed at appropriately chosen values, as in Ref. 7. The mean field is represented by a Nilsson potential with an axial deformation of $\epsilon=0.22$ for ^{165}Lu and $\epsilon=0.20$ for ^{81}Kr. A prolate deformation is appropriate for ^{81}Kr above the first backbend,[8] although this nucleus is transitional in character below the backbend. The gap parameters are chosen to

reproduce the empirical band crossing frequencies. They are $\Delta_p=\Delta_n=1.1$ MeV for ^{165}Lu, and $\Delta_p=1.23$ MeV and $\Delta_n=1.14$ MeV for ^{81}Kr. The proton Fermi level in ^{165}Lu was placed at $\lambda_p=5.85\hbar\omega_0$ so as to reproduce the small splitting observed experimentally[9] between the $K^\pi=\frac{9}{2}^-$ and $\frac{7}{2}^-$ bandheads. Otherwise, the Fermi levels were determined from the BCS equations at $\omega=0$.

The $M1$ operator in units of the nuclear magneton (μ_N) is

$$\theta_\nu^{M1}(\omega)=\left[\frac{3}{4\pi}\right]^{1/2}\{[g_l-g_R(\omega)]\hat{l}_\nu+[g_s-g_R(\omega)]\hat{s}_\nu\}\ , \tag{3}$$

where $\hat{l}_\nu$ and $\hat{s}_\nu$ are the single-particle orbital angular momentum and intrinsic spin operators, respectively, $g_l=1$ for protons and 0 for neutrons, and $g_s=0.7\times g_s$(free nucleon)$=3.91$ for protons and -2.67 for neutrons. The core g factor is obtained from the cranking wave functions for each ω as[10,11]

$$g_R(\omega)=\frac{g_l^{(n)}L_x^{(n)}+g_s^{(n)}S_x^{(n)}+g_l^{(p)}L_x^{(p)}+g_s^{(p)}S_x^{(p)}}{J_x^{(n)}+J_x^{(p)}}\ , \tag{4}$$

where the neutron orbital angular momentum is

$$L_x^{(n)}=\sum_{i\nu\mu}\langle\nu|\hat{l}_x|\mu\rangle B_\nu^{*i}B_\mu^i\ , \tag{5}$$

and so forth. The $M1$ reduced transition matrix elements are then obtained as[6,12]

$$B(M1;I,\alpha,i\to I\pm1,-\alpha,f)=\left|{}_f\left\langle-\alpha\left|\frac{1}{\sqrt{2}}(i\theta_y^{M1}\mp\theta_z^{M1})\right|\alpha\right\rangle_i\right|^2\ , \tag{6a}$$

$$B(M1;I,\alpha,i\to I,\alpha,f)=|{}_f\langle\alpha|\theta_x^{M1}|\alpha\rangle_i|^2\ . \tag{6b}$$

The present calculations were carried out using a basis of three harmonic oscillator shells for each kind of particle.

B. The particle-rotor model

In order to compare with the cranking model, we also study the particle-rotor model for ^{165}Lu. When both the odd proton quasiparticle and the aligning $i_{13/2}$ neutron quasiparticles responsible for backbending are treated explicitly, this model contains all the effects of many-body three-dimensional angular momentum coupling that were emphasized in Refs. 2–4.

The three-quasiparticle plus rotor calculation is made in two steps. First, the particle-rotor Hamiltonian of the doubly even core,

$$H_c=\theta_I^{-1}\mathbf{R}^2+\tfrac{1}{8}C(\theta_I-\theta_0)^2+\sum_\nu(\epsilon_\nu-\lambda_n)a_\nu^\dagger a_\nu+\tfrac{1}{2}\Delta_n\sum_{\nu\mu}\delta(\bar{\nu},\mu)(a_\nu^\dagger a_\mu^\dagger+a_\mu a_\nu)\ , \tag{7}$$

is diagonalized in the space of rotor core plus zero or two $i_{13/2}$ BCS quasiparticles. This Hamiltonian and its solution is described in more detail in Ref. 13. $\mathbf{R}$ is the rotor core angular momentum, $\mathbf{I}$ is the total angular momentum, and $\frac{1}{2}\theta_I$ is a rotational moment of inertia which is determined for each I by the variable moment of inertia (VMI) method. The splitting of the $i_{13/2}$ suborbitals is the same as in Ref. 13. The VMI parameters, $C=0.002\,575$ MeV^3 and $\theta_0=18.172$ MeV^{-1}, and the pairing parameters, $\lambda_n=0.037$ MeV above the $\Omega=\frac{3}{2}$ suborbital and $\Delta_n=0.796$ MeV, were adjusted to reproduce the experimental[14] yrast levels of ^{166}Hf up through the first backbend. It was not possible to simultaneously fit the moment of inertia of the S band, which becomes too large in the present calculation. The calculated and experimental yrast lines of ^{166}Hf are compared in Fig. 1, where the quantities I_x and ω on the axes are obtained as functions of I from the energy levels using the relations[7]

$$I_x(I)=[(I+\tfrac{1}{2})^2-K^2]^{1/2}\ , \tag{8}$$

$$\omega(I)=[E(I+1)-E(I-1)]/[I_x(I+1)-I_x(I-1)]\ . \tag{9}$$

Here, K is the spin of the band head for $K=0$ or $\Delta I=1$ bands.

The $M1$ operator is the same as in Eq. (3). However, the single-particle space is now restricted to the $\nu i_{13/2}$ shell, while g_R refers to the "naked" core excluding the $\nu i_{13/2}$ shell and is a constant, since the rotational alignment takes place outside the core. The g factor for the naked core should be larger than for the whole nucleus in the ground band, because a substantial part of the neutron contribution to rotation comes from the valence $\nu i_{13/2}$ shell. With $g_R=0.41$ for the naked core, the particle-rotor calculation reproduces the g factor of the 2^+ state of ^{166}Hf that was derived microscopically using the cranking model, $g(2^+)=0.31$. The intrinsic $E2$ moment of the core is set equal to 5.9 e b, in order to reproduce the experimental[15] $B(E2;2^+\to0^+)$ for ^{166}Hf.

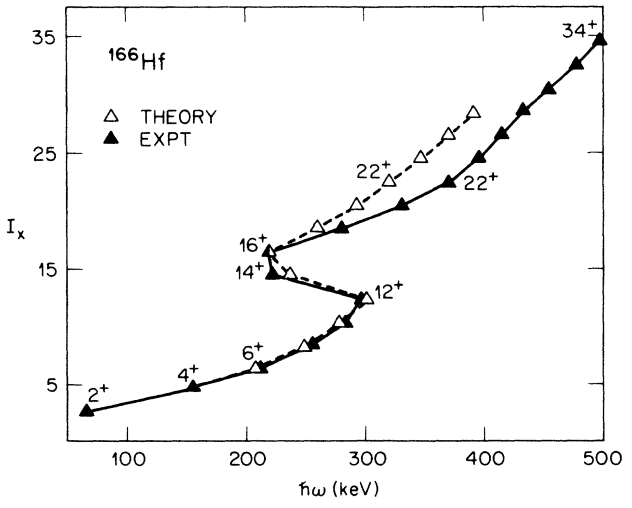

FIG. 1. The yrast energy levels from the two-quasiparticle plus rotor calculation for ^{166}Hf (open triangles) are compared with the experimental levels (Ref. 14) (solid triangles) in a plot of aligned angular momentum I_x [Eq. (8)] vs rotational frequency ω [Eq. (9)].

In the second step of the coupling calculation, the odd proton is coupled to a core consisting of the neutron $i_{13/2}$ shell plus the rotor. The Hamiltonian is[16]

$$H = H_c + \sum_{j\nu} (\epsilon_j - \lambda_p) a^\dagger_{j\nu} a_{j\nu} + \tfrac{1}{2}\Delta_p \sum_{j\nu\mu} \delta(\bar{\nu},\mu)(a^\dagger_{j\nu} a^\dagger_{j\mu} + a_{j\mu} a_{j\nu}) - \kappa \mathbf{q}\cdot\mathbf{Q} , \quad (10)$$

where the single-particle energies ϵ_j and creation operators $a^\dagger_{j\nu}$ are for spherical j shells, $\mathbf{q}$ is the single-particle quadrupole operator, and $\mathbf{Q}$ is the core quadrupole operator. The $M1$ operator in this second step is the sum of the quasiproton and core $M1$ operators, with the core $M1$ matrix elements being known from the first step. The quadrupole coupling parameter κ is set equal to 2.12 MeV, which corresponds to a deformation of $\epsilon \approx 0.24$. The Hamiltonian (10) is diagonalized in a basis of spherical particle states and equivalent hole states coupled to the core states.[16]

In the present calculation of the negative-parity levels of ^{165}Lu, the single-proton basis spans the $h_{11/2}$, $h_{9/2}$, and $f_{7/2}$ shells, with $\epsilon(h_{11/2})=0$, $\epsilon(h_{9/2})=4.9$ MeV, and $\epsilon(f_{7/2})=6.0$ MeV. The energy levels of the $K^\pi = \frac{9}{2}^-$ band in ^{165}Lu, and the low-lying $K^\pi = \frac{7}{2}^-$ bandhead, are then reproduced (Fig. 2) by setting $\lambda_p = 0.45$ MeV and taking the pairing $uu + vv$ factors to power 5 to get Coriolis attenuation. The gap parameter, $\Delta_p = 0.92$ MeV, is from the odd-even mass difference. The moment of inertia above the backbend is seen to be too large, reflecting the same deficiency in the theoretical ^{166}Hf core (Fig. 1). The advantage of the two-step procedure is that it is not necessary to include all the core states in the second step. It turned out that the even-spin yrast and yrare levels of the core were sufficient to obtain convergence for the energies and $M1$ properties of the odd-mass yrast levels, which greatly reduced the dimension of the numerical problem.

Results are also presented below for particle-core coupling of the odd proton to the yrast levels only. Then the core quadrupole matrix elements were taken from the rotational model.[17] If the $i_{13/2}$ shell plus rotor quadrupole matrix elements were to be used in coupling to the yrast states only, the energy levels of the odd-mass system would exhibit unphysical behavior in the band crossing region.

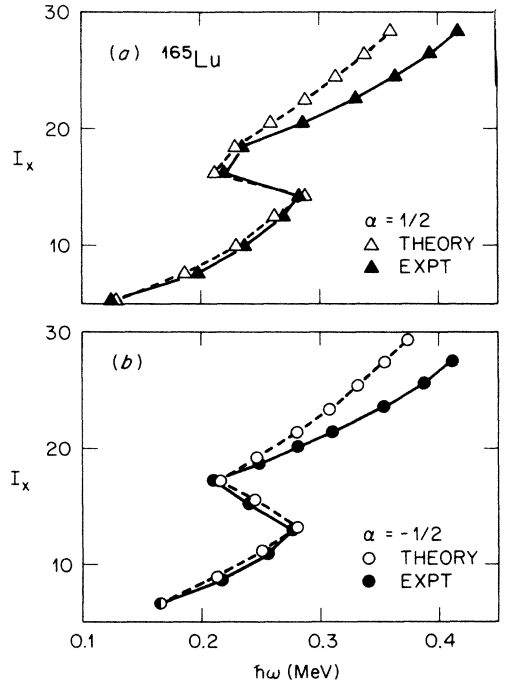

FIG. 2. (a) The yrast energy levels of signature $\alpha = +\frac{1}{2}$ from the three-quasiparticle plus rotor calculation for ^{165}Lu (open triangles) and the experimental levels (Ref. 9) (solid triangles) in a plot similar to that of Fig. 1. (b) Same as (a), but for signature $\alpha = -\frac{1}{2}$.

III. RESULTS

A. Core g factors

Before looking at the results for odd-mass systems, let us consider the underlying even-even cores. The g factors for the yrast states of ^{166}Hf obtained from the cranking and two-quasiparticle plus rotor models are plotted in Fig. 3. Also shown in Fig. 3 is the curve resulting from a simple formula proposed by Frauendorf,[18]

$$g = g_R + (g_j - g_R) i/I , \quad (11)$$

where g_R refers to the ground (or reference) band, i is the aligned angular momentum, and g_j is the single-particle g factor of the j shell in which alignment occurs. Here, $g_j = -0.20$ for the $\nu i_{13/2}$ shell[18] and $g_R = 0.31$. Using the standard method[7] of extracting i from the observed energy levels, it is found that i increases from 0 in the ground band to $10\hbar$ in the S band.

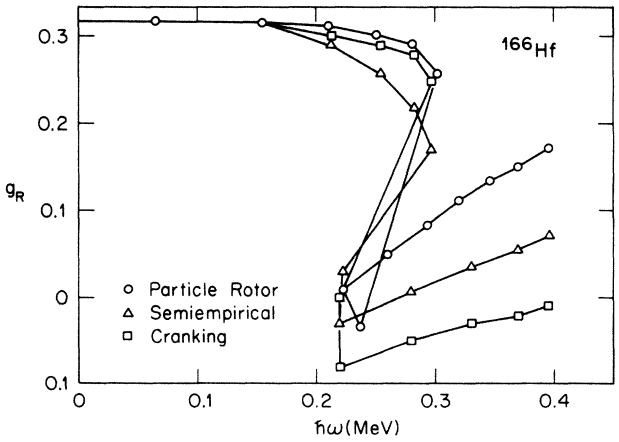

FIG. 3. Calculated g factors for the yrast states of ^{166}Hf. The squares are from the cranking model, with a proper treatment of band mixing in the band crossing region, the circles are from the two-quasiparticle plus rotor model, and the triangles were obtained using the simple formula (11).

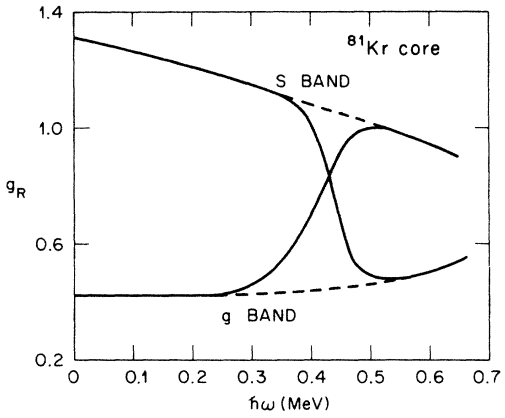

FIG. 4. The g factors of the ^{81}Kr core obtained directly from the cranking model as a function of rotational frequency, ω, for the yrast states (lower curve at low ω) and the two-quasiproton yrare states (upper curve at low ω). The dashed curves are drawn by hand to connect the yrast and yrare sections of the unperturbed ground and S bands, which cross and mix at $\hbar\omega \approx 0.28$ MeV.

Comparing the curves in Fig. 3, it is seen that particle-rotor curve slopes up more steeply than the others at high ω. One contributing factor to this when plotting versus ω instead of I is simply that the particle-rotor calculation overestimated the moment of inertia of the S band. Otherwise, the curves in Fig. 3 are quite similar, and demonstrate the dominant role of the aligned angular momentum i as implied by the simple formula (9).

The alignment of $i_{13/2}$ neutrons leads to a decrease of the g factor (Fig. 3). An increase of the g factor would follow from the alignment of $g_{9/2}$ protons ($g_j = 1.32$), which is believed to occur in ^{81}Kr. This can be seen in Fig. 4, which shows cranking results for the ^{81}Kr core. The cranking model g factors of both the yrast and the yrare level sequences are plotted in Fig. 4. The change of the g factor in the yrast sequence is then seen to occur because the yrast and yrare levels exchange character around $\hbar\omega = 0.42$ MeV. Within this band crossing region, the cranking results should not be interpreted literally[19] because band mixing in the cranking model occurs between states of equal ω instead of equal I. The cranking calculation in the crossing region must be supplemented by a band mixing analysis as described in Ref. 20. The g factors of the unmixed ground and S bands would be needed to obtain g factors from such a band mixing analysis. These pure configuration g factors can be constructed graphically as indicated by the dashed curves in Fig. 4. The cranking results in Fig. 3 for ^{166}Hf were, in fact, obtained by this procedure.

B. $M1$ rates in ^{165}Lu

Results from the different calculations of $B(M1)$ rates in the $K^\pi = \frac{9}{2}^-$ yrast band of ^{165}Lu are summarized in Fig. 5. Figure 5(a) shows "experimental" values, extracted from the measured branching ratios[9,21] using calculated $B(E2)$ rates from the three-quasiparticle plus rotor calculation. The $B(M1)$ rates in Fig. 5(a) are lower than those given in the experimental papers, where $B(E2)$ rates were obtained using the rotational model and an enlarged quadrupole moment. However, lifetime measurements in the isotone ^{168}W indicate that no such enlargement over the quadrupole moment of the 2^+ state occurs for the high spin states.[22] Furthermore, a few $B(E2)$ rates in the backbending region of ^{165}Lu are strongly suppressed relative to the rotational model due to band mixing, and the extracted $B(M1)$ rates in Fig. 5(a) are correspondingly reduced. Figure 5(a) also shows the $B(M1)$ rates given by the strong coupling rotational model formula:[17]

$$B(M1; KI \rightarrow KI-1) = 3/4\pi (g_K - g_R)^2 K^2 \langle IK\,10 \mid I-1K\rangle^2 \mu_N^2 ,$$
$$g_K = g_l + (g_s - g_l)\langle K \mid \hat{s}_z \mid K\rangle . \quad (12)$$

Here, $K = \frac{9}{2}$, $\langle K \mid \hat{S}_z \mid K\rangle \approx \frac{9}{22}$ is obtained from the $\Omega = \frac{9}{2}$ Nilsson orbit from the $h_{11/2}$ shell, and g_R is from the cranking model (Fig. 3). Strong coupling is seen to grossly overestimate the $B(M1)$ rates, which demonstrates the necessity of taking the nonadiabaticity of the odd quasiproton into account, either by cranking or by particle-core coupling.

Figure 5(b) shows results of the present cranking model for the unmixed bands. The $B(M1)$ rates are still too high at low ω, but reproduce the experimental values quite well for the highest spin states. This is one of the main results of the present paper. Regarding low ω, Dönau[5] has demonstrated that the cranking $B(M1)$ rates can be improved by including various K dependences neglected in Eqs. (3) and (6). One of these simply corresponds to multiplying the cranking $B(M1)$ rates by $2\langle IK\,10 \mid I-1K\rangle^2$.

Figure 5(c) shows the $B(M1)$ rates from the three-quasiparticle plus rotor calculation. This model is an interesting reference because it embodies three-dimensional, quantum mechanical coupling of the angular momenta of the rotor, the neutron $i_{13/2}$ configuration, and the proton quasiparticle. The $B(M1)$ rates in Fig. 5(c) are higher in the three-quasiparticle band than in the one-quasiparticle band, and the signature splitting continues to increase with increasing ω. This is contrary to the results of the supposedly equivalent three-quasiparticle plus rotor calculation in Ref. 3, but in agreement with the expectations of Ref. 4. The agreement with the data in Fig. 5(a) is excellent at lower spins where the experimental error bars are small. Let us focus on the differences between Figs. 5(a) and 5(c).

First, it may be noted that whereas the calculated $B(M1)$ from the $\frac{33}{2}$ level is suppressed as in the data, the calculated $B(M1)$ from the $\frac{35}{2}$ level is not. This could be because transition rates at the band crossing are very sensitive to detail. For example, the two-quasiparticle plus rotor fit to ^{166}Hf (Fig. 1) reproduces the experimental estimate of the relative transition intensities from the 14^+ level to the two observed 12^+ levels, which corresponds to a ~ 4 times larger $B(E2)$ rate than the yrare 12^+ level. However, we found that other equally good fits to the

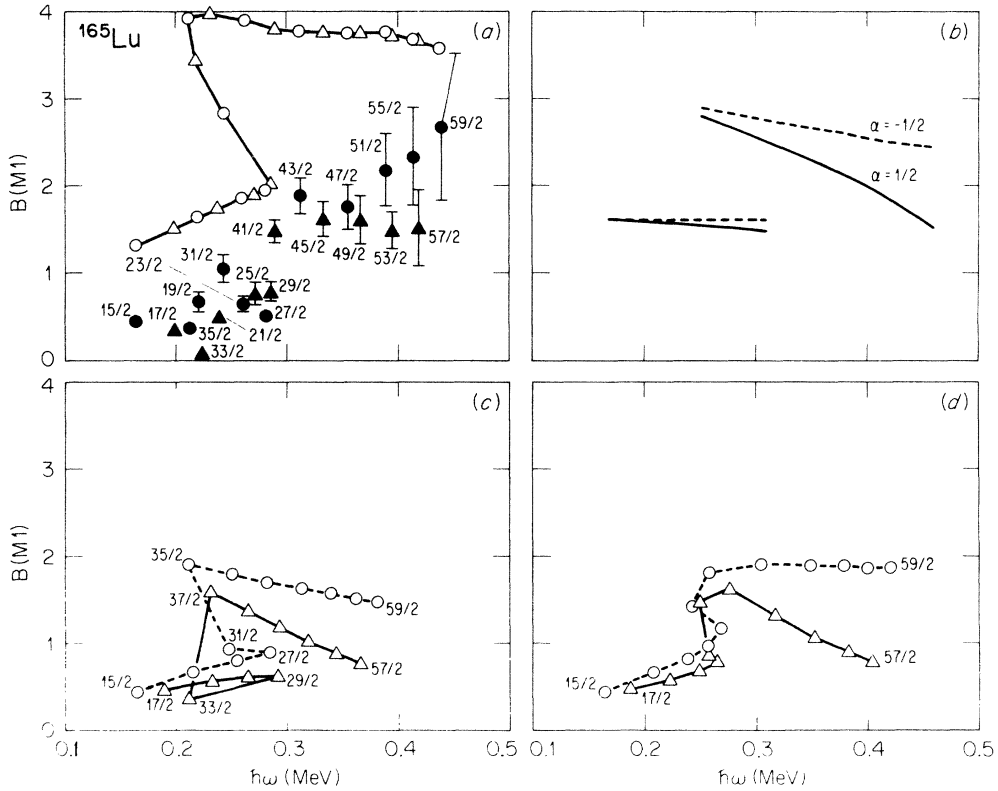

FIG. 5. $B(M1)$ transition rates in μ_N^2 from states in the $\alpha=\frac{1}{2}$ (triangles and solid curves) and $\alpha=-\frac{1}{2}$ (circles and dashed curves) yrast levels of ^{165}Lu. (a) Experimental data (Refs. 9 and 21) (solid symbols) and the strong-coupling model (open symbols). (b) The cranking model. (c) The three-quasiparticle plus rotor model. (d) One-quasiparticle coupling to a core with the cranking model g factors.

^{166}Hf energies gave very different results, and could also alter the ^{165}Lu levels at the band crossing.

A second difference is that the $B(M1)$ rates in Fig. 5(c) appear to become lower than the experimental ones at the highest ω's. Regarding the data, it may be emphasized that the statistical error bars are large, and that a decrease of the $B(E2)$ rates at high spins such as that observed, for example, in ^{160,161}Yb and ^{172}W (Refs. 23 and 24) could produce a similar decreasing trend in the "experimental" $B(M1)$ rates. The $B(M1)$ rates could also be affected by even a small amount of triaxiality.[4] Regarding Ref. 4, it may be noted that the $B(M1)$ rates from the triaxial particle-rotor-like model used there are consistently higher than ours. This would have resulted if the Fermi level λ_p was placed slightly close to the $K=\frac{9}{2}$ Nilsson orbit (Ref. 4 does not present the fit to the energy levels). The $B(M1)$ rates in both our particle-rotor and cranking calculations are highly sensitive to such an increase of λ_p.

Next, we consider the differences between our particle-rotor and cranking results [Figs. 5(c) and 5(b)]. The lower $B(M1)$ rates and larger signature splitting in Fig. 5(c) represents a real difference between the models, since the physical input is almost identical. The difference at high ω is not just due to the different behavior of the core g factors seen in Fig. 3. This point can be proved by coupling the odd proton to a core consisting of the yrast states only. The one-quasiparticle plus yrast rotor states is still a good approximation to the full calculation except in the band crossing region. Figure 5(d) shows the results of such a calculation, with the experimental ^{166}Hf yrast energies and the cranking model g factors $g_R(\omega)$ from Fig. 2. The $B(M1)$ rates in Fig. 5(d) are more similar to those of three-quasiparticle plus rotor model [Fig. 5(c)] than the cranking model [Fig. 5(b)].

An approach similar to that of Fig. 5(d) was previously studied in Ref. 3. There it was found to give a gradual increase of the $B(M1)$ rates over a much wider region of spin around the band crossing than is observed in experiment. This poor result was obtained because the cranking model was interpreted literally in the band-crossing region. Thereby, too many angular momentum states were described as strongly band mixed, and the change in the core g factor was spread out over all these states.

C. $M1$ rates in ^{81}Kr

In Fig. 6 cranking model results are compared with the experimental[8] $B(M1)$ rates in ^{81}Kr. These are the best available data that involve a band crossing caused by proton alignment. As in Fig. 5(b), a cranking model description of the band crossing region has been circumvented by plotting results for the unmixed ground and S bands, obtained here by taking the core g factors given by the dashed curves in Fig. 4. The prediction for states in the band-crossing region is then that they should have $B(M1)$ rates somewhere below the upper curve, dashed or solid

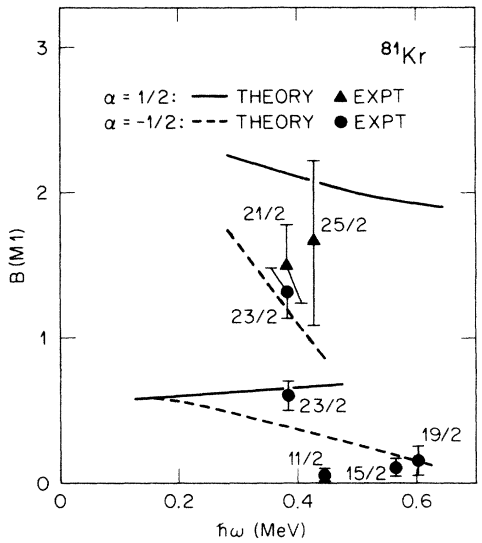

FIG. 6. $B(M1)$ transition rates in ^{81}Kr. The solid circles and triangles are experimental data (Ref. 8) for $\alpha=-\frac{1}{2}$ and $\frac{1}{2}$, respectively. There are two different measurements for $I=\frac{23}{2}$. The dashed and solid curves are cranking model results for $\alpha=-\frac{1}{2}$ and $\frac{1}{2}$, respectively. The lower pair of curves is for the unperturbed ground state and the upper pair is for the unperturbed proton-aligned S band.

for the two signatures. The $\frac{23}{2}$ level lies near or below the upper dashed curve, and the $\frac{21}{2}$ and $\frac{25}{2}$ levels lie in between the two solid curves. The observed increase of the $M1$ rates due to proton alignment is thus compatible with the cranking results.

IV. SUMMARY

The purpose of this work has been to investigate how well strong $M1$ transitions at high spin can be described by the cranking method proposed in Sec. II A. According to this method, both the quasiparticle transition matrix element and a g factor for the rest of the nucleus are to be calculated from the cranking model wave functions.

The most relevant experimental data for testing the method comes from recent measurements[9,21] on ^{165}Lu. There the $\Delta I=1$ transitions are observed up to high spin, in part presumably because the core g factor undergoes major changes associated with rotational alignment of high-j quasiparticles, and in part because K is large. It is for large K that the cranking model $M1$ rates are expected to be least accurate.[5] Furthermore, ^{165}Lu is expected to have an approximately axial shape. The cranking results were also compared with core-quasiparticle coupling calculations where angular momentum is handled properly. We note that previous studies of both three-quasiparticle plus core coupling and one-quasiparticle plus core coupling in Ref. 3 appear to be seriously flawed.

The assumption of the cranking formalism that the role of the core is completely contained in an ω-dependent g factor is supported by one-quasiparticle plus core coupling calculations like the one in Fig. 5(d). There the core consists of a single $\Delta R=2$ band, so the g factors are the only core $M1$ matrix elements entering the calculation, but the resulting $M1$ rates are nevertheless similar to those obtained with a two-quasiparticle plus rotor core. The importance of the ω (or I) dependence of the core g factor (Figs. 3 and 4) for the $M1$ rates is obvious in both ^{165}Lu (Fig. 5, proton transitions and neutron alignment) and ^{81}K (Fig. 6, neutron transitions and proton alignment).

The cranking quasiparticle transition matrix elements are generally an improvement over strong coupling [Fig. 5(b) versus the theoretical curve in Fig. 5(a); the cranking $M1$ rates at the very lowest spins can be brought down by applying the factor $2\langle IK10\,|\,I-1K\rangle^2$]. At the highest spins the discrepancy between the cranking model and experiment vanishes, perhaps fortuitously, while the discrepancy between the cranking and three-quasiparticle plus rotor models is less than a factor of 2. These results indicate that the cranking model of Sec. II A should be a useful tool for evaluating $M1$ data from quasicontinuum spectroscopy.

ACKNOWLEDGMENTS

The Joint Institute for Heavy Ion Research has as member institutions the University of Tennessee, Vanderbilt University, and the Oak Ridge National Laboratory; it is supported by the members and by the Department of Energy through Contract No. DE-AS05-76ER0-4936 with the University of Tennessee. UNISOR is a consortium of ten institutions, supported by them and by the Office of Energy Research of the U.S. Department of Energy under Contract No. DE-AC05-76OR00033 with Oak Ridge Associated Universities.

*Permanent address: Institute of Atomic Energy, Beijing, People's Republic of China.

[1]P. Ring and P. Schuck, in *The Nuclear Many-Body Problem* (Springer, New York, 1980).
[2]F. Dönau and S. Frauendorf, in *High Angular Momentum Properties of Nuclei,* edited by N. R. Johnson (Harwood, New York, 1982), p. 143.
[3]E. M. Müller and U. Mosel, Phys. Lett. **160B**, 21 (1985).
[4]I. Hamamoto and B. Mottelson, Phys. Lett. **167B**, 370 (1986).
[5]F. Dönau, Zentralinstitut für Kernforschung Rossendorf, Dresden, German Democratic Republic, report, 1985 (unpublished).
[6]Y. S. Chen and I. Hamamoto, Phys. Scr. **24**, 763 (1981).
[7]R. Bengtsson and S. Frauendorf, Nucl. Phys. **A327**, 139 (1979).
[8]L. Funke, F. Dönau, J. Döring, P. Kemnitz, E. Will, G. Winter, L. Hildingsson, A. Johnson, and Th. Lindblad, Phys. Lett. **120B**, 301 (1983).
[9]S. Jonsson, J. Lyttkens, L. Carlén, N. Roy, H. Ryde, W. Walus, J. Kownacki, G. B. Hagemann, B. Herskind, J. D. Garrett, and P. O. Tjøm, Nucl. Phys. **A422**, 397 (1984).
[10]M. Diebel, A. N. Mantri, and U. Mosel, Nucl. Phys. **A345**, 72 (1980).
[11]Y. S. Chen and S. Frauendorf, Nucl. Phys. **A393**, 135 (1983).
[12]I. Hamamoto and H. Sagawa, Nucl. Phys. **A327**, 99 (1979).

[13]J. Almberger, I. Hamamoto, and G. Leander, Phys. Scr. **22**, 331 (1980).

[14]H. Hübel, K. P. Blum, K. H. Maier, A. Maj, H. Kluge, A. Kuhnert, J. Recht, and M. Guttormsen, in *Proceedings of the XXIIIrd International Winter Meeting on Nuclear Physics, 1985,* edited by I. Iori (University of Milan, Milan, 1985).

[15]B. Bochev, S. Iliev, R. Kolpakchieva, S. A. Karamian, T. Kutsarova, E. Nadjakov, and Ts. Vendova, Nucl. Phys. **A282**, 159 (1977).

[16]F. Dönau and S. Frauendorf, Phys. Lett. **71B**, 263 (1977).

[17]A. Bohr and B. R. Mottelson, in *Nuclear Structure* (Benjamin, New York, 1975), Vol. 2.

[18]S. Frauendorf, Phys. Lett. **100B**, 219 (1981).

[19]I. Hamamoto, Nucl. Phys. **A271**, 15 (1976).

[20]R. Bengtsson and S. Frauendorf, Nucl. Phys. **A314**, 27 (1979).

[21]P. Frandsen, J. D. Garrett, G. B. Hagemann, B. Herskind, R. Chapman, J. C. Lisle, J. N. Mo, L. Carlén, J. Lyttkens, H. Ryde, P. M. Walker, and M. Riley, in Proceedings of the Symposium on Electromagnetic Properties of High Spin States, Research Institute for Physics, Stockholm, 1985, edited by I. Berström (unpublished).

[22]G. D. Dracoulis, G. D. Sprouse, O. C. Kistner, and M. H. Rafailovich, Phys. Rev. C **29**, 1576 (1984).

[23]M. P. Fewell, N. R. Johnson, F. K. McGowan, J. S. Hattula, I. Y. Lee, C. Baktash, Y. Schutz, J. C. Wells, L. L. Riedigner, M. W. Guidry, and S. C. Pancholi, Phys. Rev. C **31**, 1057 (1985).

[24]M. N. Rao *et al.*, Bull. Am. Phys. Soc. **30**, 1275 (1985); submitted to Phys. Rev. Lett.